Nephrol Dial Transplant (2014) 29: 2235–2243
doi: 10.1093/ndt/gfu324
Advance Access publication 5 November 2014

ndt
Nephrology Dialysis Transplantation

Original Articles

Severe vascular calcification and tumoral calcinosis in a family with hyperphosphatemia: a fibroblast growth factor 23 mutation identified by exome sequencing

Anuja Shah[1,*], Clinton J. Miller[2,*], Cynthia C. Nast[3], Mark D. Adams[4], Barbara Truitt[2], John A. Tayek[5], Lili Tong[1], Parag Mehtani[1], Francisco Monteon[6], John R. Sedor[7], Erica L. Clinkenbeard[8], Kenneth White[8], Rajnish Mehrotra[1], Janine LaPage[1], Patricia Dickson[9], Sharon G. Adler[1,**] and Sudha K. Iyengar[2,**]

[1]Division of Nephrology and Hypertension, Los Angeles Biomedical Research Institute at Harbor-UCLA Medical Center, Torrance, CA 90502, USA, [2]Department of Epidemiology and Biostatistics, Case Western Reserve University School of Medicine, Cleveland, OH 44106, USA, [3]Division of Pathology, Los Angeles Biomedical Research Institute at Harbor-UCLA Medical Center, Torrance, CA 90502, USA, [4]J. Craig Venter Institute, San Diego, CA 92121, USA, [5]Division of General Internal Medicine, Los Angeles Biomedical Research Institute at Harbor-UCLA Medical Center, Torrance, CA 90502, USA, [6]Unidad de Nefrologia y Transplante, Hospital Mexico-Americano, Guadalajara, Jalisco, Mexico, [7]Department of Medicine, MetroHealth Medical Center, Cleveland, OH 44109, USA, [8]Department of Medical and Molecular Genetics, Indiana University School of Medicine, Indianapolis, IN 46202, USA and [9]Division of Medical Genetics, Los Angeles Biomedical Research Institute at Harbor-UCLA Medical Center, Torrance, CA 90502, USA

Correspondence and offprint requests to: Sharon G. Adler; E-mail: sadler@labiomed.org
[*]A.S. and C.J.M. contributed equally to this work.
[**]S.G.A. and S.K.I. contributed equally to this work.

ABSTRACT

Background. Tumoral calcinosis is an autosomal recessive disorder characterized by ectopic calcification and hyperphosphatemia.
Methods. We describe a family with tumoral calcinosis requiring amputations. The predominant metabolic anomaly identified in three affected family members was hyperphosphatemia. Biochemical and phenotypic analysis of 13 kindred members, together with exome analysis of 6 members, was performed.
Results. We identified a novel Q67K mutation in fibroblast growth factor 23 (FGF23), segregating with a null (deletion) allele on the other FGF23 homologue in three affected members. Affected siblings had high circulating plasma C-terminal FGF23 levels, but undetectable intact FGF23 or N-terminal FGF23, leading to loss of FGF23 function.
Conclusions. This suggests that in human, as in experimental models, severe prolonged hyperphosphatemia may be sufficient to produce bone differentiation proteins in vascular cells, and vascular calcification severe enough to require amputation. Genetic modifiers may contribute to the phenotypic variation within and between families.

Keywords: FGF23, hyperphosphatemia, vascular calcification

INTRODUCTION

Calcium and phosphorus homeostases are required for proper bone formation; alterations have been linked to vascular calcification. Incorporation of calcium and phosphorus into hydroxyapatite and osteoblastic transformation of vascular smooth muscle cells are tightly regulated processes. In chronic kidney disease (CKD) and end-stage renal disease (ESRD), the

relative roles of hyperparathyroidism, hyperphosphatemia, vitamin D therapy, calcium homeostasis and the uremic milieu contributing to vascular calcification are not completely understood. Since vascular injury contributes to significant morbidity and mortality in these settings, its pathogenesis is an active area of clinical and experimental research [1, 2].

Fibroblast growth factor 23 (FGF23) is produced in osteoblasts/osteocytes and has a central role in regulating calcium–phosphate metabolism [3]. FGF23 decreases proximal tubule expression of the sodium–phosphate cotransporters NPT2a and NPT2c, inducing phosphaturia. 1,25$(OH)_2$ vitamin D stimulates FGF23 synthesis, likely through binding to the FGF23 promoter. Additionally, in a negative feedback loop, FGF23 decreases 1α-hydroxylase activity impairing calcitriol synthesis and increases 24-hydroxylase activity causing calcitriol degradation, secondarily reducing gastrointestinal phosphate absorption. Thus, FGF23 is the most important direct effector of phosphate balance known [1, 2]. We report a family with tumoral calcinosis (TC) with an atypical phenotype of severe vascular calcification requiring amputation. An FGF23 mutation inherited in compound heterozygosity with a null allele was identified along with marked hyperphosphatemia. In the absence of other vascular calcification risk factors, hyperphosphatemia was the predominant metabolic abnormality identified to explain the severe vascular calcification.

ORIGINAL ARTICLE

MATERIALS AND METHODS

Subjects

The study was reviewed and approved by the Los Angeles Biomedical Research Institute Institutional Review Board. After obtaining informed consent, blood samples from family members were processed for measurements and for DNA extraction and analysis. Full exome sequencing was performed on DNA extracted from lymphocytes, with confirmation using Sanger sequencing. DNA from the selected individuals was sheared and selectively amplified using the Agilent SureSelect Human Whole Exon 50 Mb capture kit according to the manufacturer's protocol. Each enriched library was sequenced on its own lane of an Illumina GAII sequencer. The sequencing metrics were determined using the HSmetrics ultility from the Picard software package.The mean bait coverage ranged from 102× to 134× of the sequenced exome. A CLIA-certified confirmatory analysis was performed from DNA extracted from a buccal DNA preparation on the proband only. The 13 living family members (Figure 2) were genotyped, using the Affymetrix Genome-Wide Human SNP Array 6.0 in the Genotyping and Gene Expression Core at Case Western Reserve University using standard methods. Genotype quality was assessed by calculating the random Contrast QC, which ranged from 1.03 to 3.59 with an average of 2.71, and the QC Call Rate, which ranged from 89.74 to 99.37% with an average of 97.81%.

Immunohistochemistry

Formalin-fixed sections from the proband's amputation were baked and then run on automated immunohistochemistry instruments using the following antibodies and detection systems. Primary antibodies included osteonectin (Leica, IL, USA; 1 : 100) pretreated with low pH, and tartrate-resistant acid phosphatase (TRAP; Leica, IL, USA; predilute) pretreated with high pH, both run on Leica bond III using DAB detection; and smooth muscle actin (Leica, IL, USA; prediluted) without pretreatment, CD34 (Epitomics, CA, USA; 1 : 100) pretreated with high pH and CD163 (Leica, IL, USA 1 : 100) pretreated with high pH, all run on Ventana Ultra using Ultraview Red detection. After staining, all slides were counterstained with Mayer's hematoxylin and bluing reagent.

Genotyping and loss of heterozygosity analysis

The data were loaded into Affymetrix Genotyping Console and genotypes called using the default settings. The samples were also analyzed for loss of heterozygosity (LOH) using the Genotyping Console's default settings. The regions identified in each sample were compared to determine which regions were found in affected family members but not in unaffected members. Only one region was found in the proband and affected siblings but in no other family member (Figure 4). The overlapping region from the three samples was on 12p13 between 1078103 and 6323300. The affected individuals shared the same homozygous genotypes in this region while the unaffected father and brothers had a differing genotype on both the Affymetrix array and in the exome sequencing data, confirming the LOH. The size of this region indicates that the affected individuals lost this portion of their maternally inherited chromosome 12. Two of the short-listed variants are in this region, including the FGF23 variant. The mutated FGF23 inherited from the father by the proband and two affected siblings would be the only copy expressed by the affected individuals given their loss of that portion of their maternally inherited chromosome.

SNP and inDel identification

Exome sequencing of the samples was done using an enriched library created, using the Agilent SureSelect Human All Exon Kit after shearing of the DNA on a CovarisTM S2 system (Covaris, Inc., Woburn, MA, USA) following the manufacturer's protocol for 200–300 bp fragments. Samples were run on two lanes of a GA Illumina sequencer. Sequencing reads passing quality control were aligned using BWA [4]. Duplicate reads were removed using Samtools rmdup, with 91% of the target bases with at least 10× coverage and >75% having over 30× coverage. The coverage at each targeted base and each targeted gene was calculated first by using the genome CoverageBed utility from the BEDTools software package to generate the coverage across the genome and then narrowing the resulting bedgraph to the targeted regions using a custom Galaxy workflow. The Unified Genotyper from the Genome Analysis Toolkit was used to call variants in the sequence data [5]. The resulting amino acid change, if any, from the variants was determined using SLATE, an in-house application. The variants were filtered to remove variants with a depth of coverage of <10, a positive-strand bias, and variants with <3 reads supporting the alternate allele.

Sequencing and genotyping concordance

The concordance between the Affymetrix 6.0 array genotype calls and the exome sequencing calls was determined by comparing the genotype calls overlapping the exome target region with the Unified Genotyper calls.

Determination of putative causative alleles

The causative allele is predicted to be rare; the variants were further filtered to remove all db SNPs from build 132 not tagged as being a clinical submission, all 1000 Genome SNPs from the pilot release and all other SNPs from an in-house database of exome sequences. The variants were further filtered to remove all synonymous mutations as identified by an in-house script. The variants shared by the proband and the two affected siblings were determined by intersecting the variant lists for each at sites where all three had sufficient coverage to call SNPs. The variants from this list not found in the unaffected father, sibling and wife were determined for each site where the unaffected individuals had sufficient coverage to call SNPs. Likewise, the variants where the unaffected father was heterozygous and the three affected siblings had a homozygous call were determined using a similar approach. Finally, variants unique to each sample were determined by removing all intersecting variants from the other samples.

Plasma FGF23 measurement

Intact plasma FGF23 measurements used a two-site enzyme-linked immunosorbent assay (Kainos Laboratories) in which monoclonal antibodies recognize full-length FGF23. 'C-terminal' FGF23 was measured by ELISA (Immutopics International), which employs polyclonal antibodies to the C-terminal domain of FGF23 (Table 3).

RESULTS

Clinical phenotype of the proband and affected and unaffected family members

The proband was referred at age 42 for hyperphosphatemia management. History was significant for below and above the knee amputations at ages 34 and 41, coronary artery calcification, tendon ossification and diverticulitis, but was negative for kidney stones or fractures. Physical examination revealed ear and digit calcified granules, cold, stiff hands with diminished finger flexion and extension, amputations and no vascular bruits. Imaging showed extensive vascular calcification involving the aorta, mesenteric, renal, carotid, limb, heart and brain vasculature along with ectopic calcification (Figure 1). Laboratory assessments demonstrated hyperphosphatemia despite normal renal function, normoalbuminuria, normal serum calcium, low parathyroid hormone (PTH) and a lack of significant hypervitaminosis D (Table 1). His total cholesterol was 171 mg/dL, triglycerides 165 mg/dL, low-density lipoprotein 83 mg/dL and high-density lipoprotein 55 mg/dL.

Two siblings had similar symptoms, one with multiple digit amputations. The pedigree in Figure 2 is a summary of the proband's family history. Affected family members had characteristics similar to the proband (two sisters TC6 and TC8 in table). The maximal tubular reabsorption of phosphate per unit volume of glomerular filtration rate (GFR) (TmP/GFR) was abnormal and high only in the affected, except for the youngest subject whose TmP/GFR was high but normal for her age. Urinary calcium tended to be higher in affected than unaffected siblings although consistently in the normal range. Serum calcium, also normal, was higher in two affected siblings than in unaffected subjects. PTH tended to be suppressed in affected family members. These features, coupled to the hyperphosphatemia, are consistent with a causative mutation in FGF23 (Table 1).

Morphology

Vessels from capillaries to medium-sized arteries were evaluated in the amputation specimen (Figure 3). Most arteriolar and small artery walls had primarily circumferential or segmental internal elastic lamina (IEL) calcification with extension toward the media. The osteocyte marker osteonectin stained capillaries and arterioles most consistently, while larger arteries showed variable staining. Arterioles and arteries, regardless of medial calcification, showed osteonectin staining in the muscularis smooth muscle cells, which retained smooth muscle actin expression. There was no extracellular osteonectin staining. There

FIGURE 1: (**A**) Extraosseus calcification is present at the right hip region (lower arrow), renal arteries and renal parenchyma (upper arrow). (**B**) Severe calcification in the abdominal aorta (arrow). (**C**) Severe calcification of cerebral vessels.

Table 1. Clinical characteristics of the proband and his affected and unaffected family members (sisters TC6 and TC8 are affected subjects)

	Proband TC2	Brother TC4	Brother TC5	Sister TC3	Father TC1	Sister TC9	Sister TC7	Sister TC6	Sister TC8	Proband's wife TC10	Son TC11	Son TC12	Daughter TC13
Phenotype	Y	N	N	N	N	N	N	Y	Y	N	N	N	N
Age	43	54	38	49	88	45	57	53	64	39	18	16	9
BMI (kg/m^2)	24.6							25.7	17.5				
Serum values													
BUN (mg/dL)	10	16	12	15	40	17	27	25	25	10	7	15	11
Creat (mg/dL)	1.2	0.97	1.02	0.65	1.1	0.9	0.9	0.6	0.8	0.56	0.77	0.71	0.54
eGFR (mL/min/1.73 m$^{2)*}$	66	88	82	97	63	68	65	105	72	121	132		
Ca (mg/dL)	9.3	8.9	9.5	9.4	9.5	9.3	9.6	9.9	10	9.4	9.5	9.5	9.5
Phos (mg/dL)	7.6	3.4	3.6	4.1	3.2	3	4	6.7	5.8	3.9	3.7	3.9	5.1
PTH (pg/mL–normal 10–65)	9	48	25	22	40	39.8	39	20	26	21	24	8	17
25-OHD3 (30–100 pg/mL)	Median value 18	17	26	19	25.5	23	11.4	27.5	6.7	21	25	33	23
1, 25-OHD3 (18–72 pg/mL)	Median value 57	24	53	Not done	42	35	33	54	73	55	64	<8	89
24-h urine results													
Creatinine, total (g)	1.4	1.91	1.1	0.82	0.86	1.04	1.15	0.47	0.68	1.19	2.53	2.37	1.19
MACR (µg/mg)	<6												
Ca	174 mg	<0.2 mg/dL	<0.2 mg/dL	<0.2 mg/dL	92 mg	96 mg	68 mg	128 mg	221 mg	<0.2 mg/dL	<0.2 mg/dL	<0.2 mg/dL	<0.2 mg/dL
Phos, total (mg)	200	264	386	386	740	650	470	240	340	369	481.6	507.6	504
TmP/GFR (mmol/L)	2.38	1.05	1.04	1.21	0.72	0.78	1.16	2.05	1.73	1.21	1.14	1.2	1.56

*Based on MDRD (not validated in those <18 years of age so not reported).

FIGURE 2: Pedigree of three generations of a family with several members affected by tumoral calcinosis. A family with three affected individuals (shaded black) was examined using both Affymetrix 6.0 genotyping array and whole-exome sequencing. All 13 living individuals were genotyped using the Affymetrix array and 6 individuals, denoted by an E, were exome-sequenced. The proband is denoted by an arrow.

were large aggregates of calcification and occasionally ossification within fibroadipose connective tissue. Immunostaining for TRAP, an osteoclast marker, showed strong expression in multinucleated cells adjacent to areas of calcification. TRAP was focally weakly positive in few macrophages and other interstitial cells, possibly fibroblasts. No vascular smooth muscle or endothelial cells stained for TRAP.

Full exomic sequencing of the proband and his affected and unaffected family members

A gene mutation in FGF23, Klotho or GALANT3 was suspected, but the prominent vascular calcification expanded our search to include potential novel mediators of vascular calcification and/or phenotypic modulators. Whole-exome sequencing was performed in six family members (proband, two affected and one unaffected sibling, his unaffected father and his wife). The proband's mother had expired, but she had no history related to vascular calcification. Her genetic sequence was imputed based on available family data. Among 17 variants that showed differences between the exomes of affected and unaffected individuals, a novel Q67K recessive FGF23 mutation was detected, which was inherited from the father in all affected siblings in compound heterozygosity with a 5.25-Mb deletion from their mother on the other allele. Not previously reported, this change is within a highly conserved N-terminal domain of FGF23, making a compelling candidate for the disease-causing mutation. The variation causing the Q67K mutation was predicted to be damaged by Polyphen2 and a likelihood ratio test [6, 7]. This variant was found to be hemizygous—confirmed by Sanger sequencing—in the three affected individuals, heterozygous in the father and unaffected sibling, and it was not found in the proband's unaffected wife. The 5.25-Mb deletion was identified via LOH analysis (Figure 4), was not present in unaffected family members and is deduced to be inherited from the mother. None of the other variants were hypothesized to be causative for TC (Table 2).

Three-dimensional structural analysis of FGF23 Q67K variant

The 3D structure of FGF23 was mutated to Q67K in a Swiss-PDB Viewer and visualized using Chimera. Supplemental

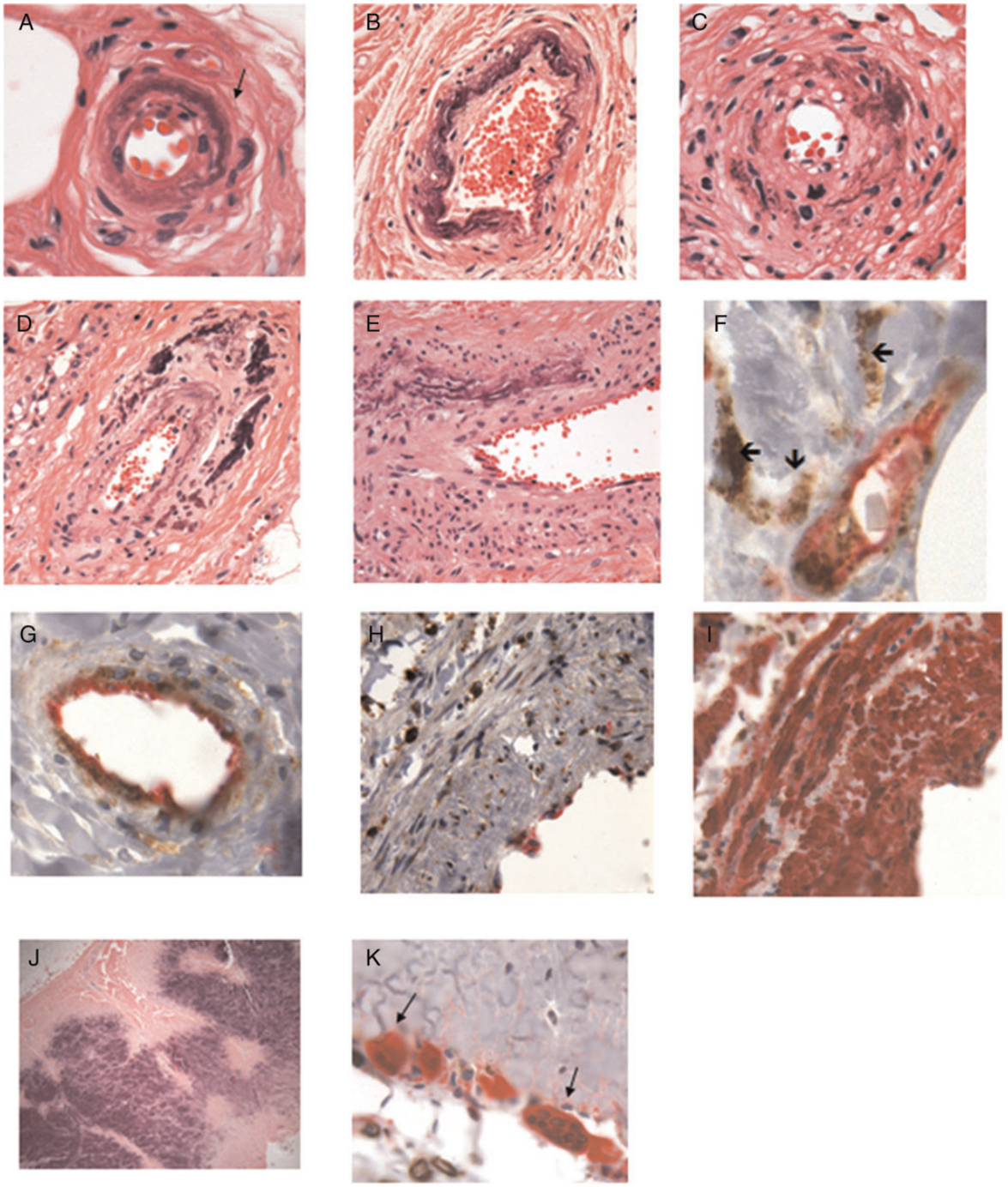

FIGURE 3: Vessels from the proband's below knee amputation. (**A**) Arteriole with circumferential calcification of elastic lamina (H&E ×400). (**B**) Artery showing circumferentially calcified internal elastic lamina (H&E ×300). (**C**) Arteriole/small artery with calcification of a portion of the internal elastic lamina that focally extends into the media (H&E ×350). (D) Small medium-sized artery with internal elastic lamina calcification and large aggregates of separate medial calcification. Fewer numbers of small- and medium-sized arteries had focal amorphous medial calcifications, ranging in size from small to involving half the artery circumference, often with focal IEL calcification (H&E ×240). (**E**) The largest medium-sized arteries had few medial calcifications (Monckeberg's calcific sclerosis) without involvement of the internal elastic lamina. No intimal calcification or fibrosis, atheromatous changes or significant inflammation were present; lipid staining for confirmation could not be performed due to paraffin embedding (H&E × 325). (**F**) Fibroadipose tissue capillary showing endothelial cells (CD34 in red) costaining for osteonectin (brown). Staining for osteonectin revealed expression in endothelial cells of capillaries, arterioles and small- and medium-sized arteries with and without calcifications. Adjacent spindle cells (arrows), likely pericytes and/or fibroblasts, also stain for osteonectin. Macrophage stain (CD163) was negative in these cells (not shown). (**G**) Small artery and (**H**) larger medium-sized artery with osteonectin (brown) in endothelium (CD34 in red) and in medial smooth muscle cells (G × 375; H × 325). (**I**) Same artery as H demonstrated preservation of smooth muscle actin staining (red) (×325). (**J**) Large focus of calcification in fibroadipose connective tissue (tumoral calcinosis) (H&E ×40). (**K**) Tartrate-resistant acid phosphatase (red) within multinucleated cells (arrows) adjacent to an area of tumoral calcinosis. Capillaries in the adjacent fibroadipose tissue are stained for CD34 (brown) (×375).

Table 2. Variants differing from affected and unaffected exome-sequenced individuals

Chr	Pos	Genotype	Variant type	RNA	Gene	SIFT pred	SIFT score	PolyPhen2 pred	PolyPhen2 score	LRT pred	LRT score	GERP score	Grantham score
chr10	121212742	C/T	M	NM_005308	GRK5	NA	0.859	NA	0.630606	D	0.999989	3.79	98
chr13	26343230	C/T	M	NM_016529	ATP8A2	D	0.98	P	0.512	N	0.936755	2.41	101
chr14	93813667	C/A	M	NM_182971	COX8C	D	0.96	P	0.693	NA	0.602624	−2.73	126
chr17	71380046	G/T	M	NM_001144952	SDK2		Not scored	B	0.001		Not Scored	3.29	94
chr17	76464861	G/C	M	NM_173628	DNAH17		Not scored	B	0.001		Not Scored	1.88	10
chr17	7722687	T/C	M	NM_020877	DNAH2	D	1	D	0.955	D	0.999997	4.02	89
chr17	79663981	C/T	M	NM_004712	HGS	D	0.99	P	0.206	N	0.317899	4.16	98
chr18	64235665	T/A	M	NM_021153	CDH19	T	0.8	B	0.041	D	1	4.69	15
chr21	43767635	G/C	M	NM_005423	TFF2	D	0.98	P	0.766	N	0.907407	2.05	10
chr4	39462537	C/T	M	NM_006859	LIAS	T	0.81	B	0.004	N	0.996043	3.32	89
chr5	147796680	A/G	M	NM_030793	FBXO38	T	0.81	D	0.985	D	0.999975	4.32	23
chr9	125281673	T/C	M	NM_001004452	OR1J4	D	0.97	D	0.993	U	0.999407	5.54	81
chr12	2968094	T/T	M	NM_021953	FOXM1	D	0.99	D	0.899	N	0.998968	4.72	38
chr12	**4488550**	**T/T**	**M**	**NM_020638**	**FGF23**	**T**	**0.44**	**D**	**0.969**	**D**	**0.999944**	**4.03**	**53**
chr14	70925832	A/A	M	NM_003813	ADAM21	D	1	D	1	U	0.967249	−2.33	29
chr17	48539903	A/C	M	NM_025149	ACSF2	T	0.75	B	0.067	N	0.752824	−0.99	76
chr8	124989850	A/A	ss	NM_001039112	FER1L6		Not scored		Not scored		Not scored	5.53	Not scored

Sisters TC6 and TC8 are affected subjects. (A) The variants found in all three affected individuals but not found in the three unaffected individuals were analyzed using SIFT, PolyPhen2, LRT, GERP and Grantham scores to predict putative effects of the variants. (B) The variants found in all three affected individuals with a genotypic difference from the unaffected father were analyzed as above. One variant at chr12:4488550 in FGF23, a gene previously reported to be involved in tumoral calcinosis, was predicted to be damaged by PolyPhen2 and a likelihood ratio test.

Figure S1 shows the wild-type FGF23 3D structure. S71, a residue previously reported to be mutated in TC patients [8], is near the Q67 variant.

Genetic modifiers

It was posited that other variants present in the affected subjects' genome might have a modifying effect. Analysis of the genotyping array and exome sequencing data showed three potential candidate genes. Haploinsufficiency of Wnt5, a gene located in the deleted region of the maternal copy of chromosome 12 in the affected individuals, is the one variation shared across all three affected siblings. The proband and one affected sibling also shared a heterozygous missense mutation in TNFRSF11B, which encodes osteoprotegerin. The proband also had a heterozygous missense mutation in SFRP1. The encoded protein, secreted frizzled-related protein 1 (SFRP1), which is upregulated in rats fed a high-phosphorous diet [9], has demonstrated interactions with Wnt proteins. No association between the phenotype severity and the potential modifiers identified secondary to the greatly varied medical care each of the affected received. This cluster of variation in genes involved in bone loss, and vascular calcification inhibition might have modified the typical hyperphosphatemic TC caused by the FGF23 mutation and may have led to more severe vascular calcification.

Circulating plasma FGF23 levels

Affected subjects had high levels of plasma C-terminal FGF23; however, intact FGF23 was undetectable by ELISA compared with carrier individuals (Table 3).This indicates that the 12p13 genomic deletion in combination with the FGF23 missense mutation resulted in the absence of circulating, intact FGF23.

DISCUSSION

We describe a family with an FGF23 mutation whose unique clinical phenotype in affected members is severe vascular calcification requiring amputations. In this family, vascular calcification, and not TC, was the most clinically significant problem. The IEL, medial and capillary vascular calcification occurred in association with hyperphosphatemia and hypophosphaturia. Overt hypercalcemia was not present, although serum calcium levels were at the upper range of normal, and there was a tendency for higher urinary calcium excretion and suppressed PTH levels. Other risk factors for vascular calcification were absent, including hyperparathyroidism, hypervitaminosis D, hypercholesterolemia, hypertension, advanced age, diabetes, albuminuria and CKD. Using exomic sequencing, a novel recessive Q67K mutation in FGF23 inherited in compound heterozygosity with a null allele was causative. This family's phenotype is unique among other reported mutations in the FGF23—αKlotho-GALNT3 spectrum of mutations causing TC because of the vascular calcification severity. The histopathologic characterization of the calcification process and the use of full exome sequencing to explore a role for genetic modifiers is also unique. These data suggest that in these patients, hyperphosphatemia appeared to be the major contributor to TC and vascular calcification severe enough to induce ischemia requiring amputations.

Intimal vascular calcification occurs in arteries of all sizes, but particularly in large- and medium-sized vessels in

atherogenesis in the general population, and in both the intima and the media in CKD and ESRD, more prominently in the media. High serum phosphorus levels have been implicated as a risk factor for vascular calcification and cardiovascular events in both groups. High serum phosphorus is associated with a higher risk of coronary artery calcification in individuals with normal renal function [10] and in these, a higher risk of death and additional cardiovascular events in patients with a prior myocardial infarction [11, 12]. In the Multi-ethnic Study of Atherosclerosis (MESA), in moderate CKD, serum phosphorus levels correlated with coronary artery and aortic calcification [13]. In ESRD, the Dialysis Outcomes and Practice Patterns Study (DOPPS) and the USRDS Wave study showed associations between serum phosphorus and calcium–phosphorus product and mortality risk [14, 15]. The evidence shows association between hyperphosphatemia, arterial stiffness, vascular calcification and left ventricular hypertrophy [16]. Thus, the distinct etiopathogenesis, localization, severity and rapidity of calcification progression in CKD and ESRD, coupled to the association between vascular calcification and mortality in this group, make understanding and preventing this process extremely important.

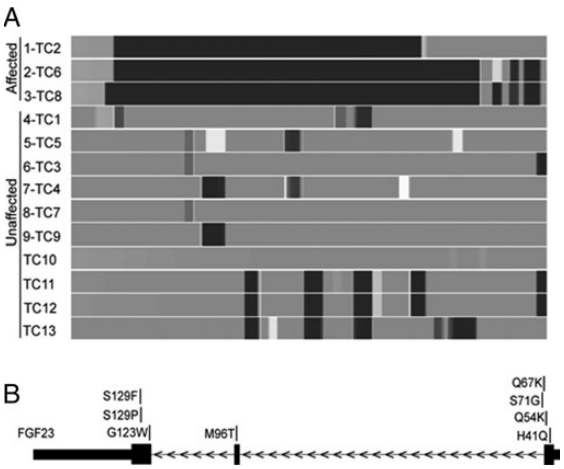

FIGURE 4: Genotyping and exome sequencing analysis of the FGF23 region. Thirteen individuals were analyzed using the Affymetrix 6.0 array and six of those were exome-sequenced. (**A**) The Affymetrix genotypes on chromosome 12 from 0 to 9 Mb were viewed using dChip. Regions of homozygosity were displayed as dark gray bars. Affymetrix's Genotyping Console identified a region in the three affected individuals that showed LOH (dark box), which contained the FGF23 gene. The cluster graphs of heterozygous calls in this region in the three affected individuals were examined and found to be miscalled by the software. The size of the region in the three affected individuals is indicative of a deletion on the maternal chromosome spanning ~5.25 Mb. Informative genotype calls from markers surrounding FGF23 were examined and individual haplotypes phased for four individuals (TC2-proband, TC5-unaffected brother, TC1-father and TC4-unaffected brother). The proband possesses one copy of the paternal allele carrying the FGF23 variant and the maternal allele with a deletion (null allele), spanning 5.25 Mb, while the two unaffected brothers carry the paternal allele carrying the variant and a maternal allele lacking the deletion. (**B**) The FGF23 variant found in the three affected individuals (top track) was viewed in USCS Genome Browser along with seven previously identified tumoral calcinosis causing variants in FGF23 (bottom track), with the variants labeled by their amino acid change. The variant from this study, Q67K, was found in a region containing three other known variants.

The proband's vascular calcification involved the media in all size arteries available for review, with smaller arteries and arterioles often showing circumferential IEL calcification. Medial calcification has been associated with CKD and ESRD. However, there is controversy regarding the relationship between IEL and medial calcification, with some investigators indicating these are independent processes and others suggesting IEL calcification precedes or initiates medial calcification [17, 18]. Prominent IEL calcification has been reported in various conditions including pseudoxanthoma elasticum, Buerger's disease and Marfan syndrome, but not hyperphosphatemia alone, a novel finding in this subject [1, 19]. Arteries and arterioles with and without calcification had endothelial and smooth muscle cell osteonectin expression, indicating osteogenic conversion. In contrast with ESRD patients, the hyperphosphatemia with normal renal function in this patient was associated with preservation of a smooth muscle morphology in vascular smooth muscle cells expressing osteocytic markers [20, 21]. These findings demonstrate some unique features of the vascular calcification where hyperphosphatemia appears to be the major contributing factor.

Vascular calcification is a highly regulated process [1]. Identification of key mediators as therapeutic or preventive targets has utility, and the role of phosphorus has been a principal object of interest [22]. Due to multiple confounders in clinical renal disease, the specific role of phosphorus in vascular calcification has been approached experimentally. After subtotal nephrectomy, rats fed a high phosphorus diet developed medial vascular calcification [9, 23], and aortic expression arrays revealed mRNAs consistent with the appearance of an osteoblast phenotype [9]. Other studies utilized targeted mutations to induce isolated hyperphosphatemia. In cultured vascular smooth muscle cells, only high phosphorus medium under

Table 3. Plasma FGF23 levels (sisters TC6 and TC8 are affected subjects)

	Proband TC2	Brother TC4	Brother TC5	Sister TC3	Father TC1	Sister TC9	Sister TC7	Sister TC6	Sister TC8	Proband's wife TC10	Son TC11	Son TC12	Daughter TC13
Phenotype	Y	N	N	N	N	N	N	Y	Y	N	N	N	N
C-terminal FGF23 (Ru/mL)	711	<50	ND	ND	204	254	ND	2020	604	ND	ND	ND	ND
Intact FGF23 (pg/mL)	0	5.96	ND	ND	14.18	50.61	33.82	0	0	ND	ND	ND	ND

the control of the sodium-dependent phosphate cotransporter, Pit-1, induced mineralization and expression of osteoblastic markers osteocalcin and Cbfa-1 [24, 25]. Pit-1 inhibition attenuated these changes [24]. In cultured endothelial cells [26], high medium phosphorus, especially with high calcium concentrations, induced apoptosis, which has been implicated indirectly in the calcification cascade in vascular smooth muscle cells and chondrocytes [27, 28]. In mice, FGF23 ablation induced hyperphosphatemia, hypercalcemia, hypervitaminosis D, suppressed PTH levels, shortened survival, soft-tissue calcification and calcified small- and medium-sized arteries reminiscent of the proband's phenotype herein. Dietary phosphorus restriction, but not vitamin D restriction, attenuated the calcification [29], implicating hyperphosphatemia as the cause. Recent data implicate FGF23 in the *inhibition* of vascular calcification in dialysis patients [30], an observation potentially congruent with our finding of circulating inactive FGF23 fragments associated with severe vascular calcification. C-terminal fragments of FGF23 (between residues 180 and 251) have been shown to competitively inhibit full-length FGF23 interactions with FGFRs and αKlotho [31]. Whether the significantly elevated C-terminal fragments observed in our TC patients potentially inhibit FGF23 or local FGFs in the vasculature, or affect vasculature and renal FGFRs differently, is currently unclear.

Five other FGF23 mutations causing TC have been described. Typical phenotypic findings included calcification around joints including hips, elbows, shoulders and knees, occasionally with diaphysitis, hyperostosis, arterial aneurysms, dental abnormalities and angioid retinal streaks [32]. Hyperphosphatemic familial TC has been associated with inappropriately high or normal vitamin D levels, and normal serum calcium [32, 33], but these cases had inconsistent vascular calcification severity. Larsson *et al.* [31] and Chefetz *et al.* [32] described missense mutations in patients with TC who demonstrated vascular calcification on imaging; no amputations were described [32, 34, 35]. FGF23 mutations were described by Araya *et al.* [33], Garringer *et al.* [34] and Masi *et al.* [36] causing TC without vascular lesions. In the family described herein, it is predicted based on the effects of the mutation that the affected subjects have circulating C-terminal FGF23 fragments incapable of receptor binding.

Varied clinical presentations despite mutations in the same gene suggest that genetic modifiers may modulate the TC phenotype. Using full exomic sequencing in this family, three potential genetic modifiers were identified that may contribute to the severity of the vascular calcification. Haploinsufficiency of Wnt5 was identified in all three affected subjects. Wnt5 haploinsufficeincy has been shown to cause bone loss [37] and associated vascular calcification in mice [38]. The expression of Wnt5a has also been shown to correlate with the severity of atherosclerosis [39]. Its role as a genetic modifier in this family remains to be determined. Two affected subjects shared a heterozygous missense mutation in TNFRSF11B, the gene-encoding osteoprotegerin. Osteoprotegerin has been implicated in vascular calcification inhibition, making it a potential gene modifier in this setting [40, 41]. Finally, the proband also had a heterozygous missense mutation in SFRP1. The regulation of SFRP1 by dietary phosphorus [9] and the known interactions between SFRP1 and Wnt signaling proteins, potentially facilitating an adaptation to inhibit calcification, also implicate this mutation as a candidate modifier of the FGF23 mutation phenotype. Thus, in the study of this family, full exomic scanning disclosed underlying genetic modifiers that may contribute to between- and within-family differences in the phenotypic expression of TC caused by the FGF23 mutation.

In conclusion, the novel FGF23 mutation in this kindred resulted in hyperphosphatemia, hypophosphaturia, arterial and capillary calcification and an ossifying cell phenotype in the absence of classical risk factors. Full genomic scanning identified potential genetic modifiers that may contribute to the phenotypic variation in vascular calcification observed. This experiment of nature supports the contention that in human, as in experimental models, hyperphosphatemia is sufficient to produce bone differentiation proteins in vascular wall cells and vascular calcification severe enough to require amputation due to ischemia.

SUPPLEMENTARY MATERIAL

Supplementary material is available online at http://ndt.oxfordjournals.org.

ACKNOWLEDGEMENTS

We acknowledge Simone Edelheit for performing the sequencing, Neal Molyneaux for assisting with the analysis of the raw sequence data and Marty Veigl and Debora Poruban for performing the experiments with the Affymetrix array and preparing the libraries for exome sequencing. This work was also supported by an anonymous donor to the Division of Nephrology and Hypertension at Harbor-UCLA. This abstract was presented at the ASN conference in November 2012. This work was funded in part by grants from the NIDDK [DK-069844 to S.G.A. and DK-063934 to K.E.W.], the Indiana Genomics Initiative (INGEN) of Indiana University, the Lilly Endowment, Inc. (K.E.W.) and DaVita Clinical Research, Inc.

CONFLICT OF INTEREST STATEMENT

None declared.

(See related article by Moe. Familial tumoral calcinosis: a valuable vehicle for discovery. *Nephrol Dial Transplant* 2014; 29: 2155–2157.)

REFERENCES

1. Demer LL, Tintut Y. Vascular calcification: pathobiology of a multifaceted disease. Circulation 2008; 117: 2938–2948
2. Chen NX, Moe SM. Vascular calcification: pathophysiology and risk factors. Curr Hypertens Rep 2012; 14: 228–237
3. Quarles LD. Skeletal secretion of FGF-23 regulates phosphate and vitamin D metabolism. Nat Rev Endocrinol 2012; 8: 276–286

4. Li H, Durbin R. Fast and accurate short read alignment with Burrows-Wheeler transform. Bioinformatics 2009; 25: 1754–1760
5. DePristo MA, Banks E, Poplin R *et al.* A framework for variation discovery and genotyping using next-generation DNA sequencing data. Nat Genet 2011; 43: 491–498
6. Adzhubei IA, Schmidt S, Peshkin L *et al.* A method and server for predicting damaging missense mutations. Nat Methods 2010; 7: 248–249
7. Chun S, Fay JC. Identification of deleterious mutations within three human genomes. Genome Res 2009; 19: 1553–1561
8. Benet-Pages A, Orlik P, Strom TM *et al.* An FGF23 missense mutation causes familial tumoral calcinosis with hyperphosphatemia. Hum Mol Genet 2005; 14: 385–390
9. Roman-Garcia P, Carrillo-Lopez N, Fernandez-Martin JL *et al.* High phosphorus diet induces vascular calcification, a related decrease in bone mass and changes in the aortic gene expression. Bone 2010; 46: 121–128
10. Foley RN, Collins AJ, Herzog CA *et al.* Serum phosphorus levels associate with coronary atherosclerosis in young adults. J Am Soc Nephrol 2009; 20: 397–404
11. Tonelli M, Sacks F, Pfeffer M *et al.* Relation between serum phosphate level and cardiovascular event rate in people with coronary disease. Circulation 2005; 112: 2627–2633
12. Dhingra R, Sullivan LM, Fox CS *et al.* Relations of serum phosphorus and calcium levels to the incidence of cardiovascular disease in the community. Arch Intern Med 2007; 167: 879–885
13. Adeney KL, Siscovick DS, Ix JH *et al.* Association of serum phosphate with vascular and valvular calcification in moderate CKD. J Am Soc Nephrol 2009; 20: 381–387
14. Tentori F, Blayney MJ, Albert JM *et al.* Mortality risk for dialysis patients with different levels of serum calcium, phosphorus, and PTH: the Dialysis Outcomes and Practice Patterns Study (DOPPS). Am J Kidney Dis 2008; 52: 519–530
15. Slinin Y, Foley RN, Collins AJ. Calcium, phosphorus, parathyroid hormone, and cardiovascular disease in hemodialysis patients: the USRDS waves 1, 3, and 4 study. J Am Soc Nephrol 2005; 16: 1788–1793
16. Kalpakian MA, Mehrotra R. Vascular calcification and disordered mineral metabolism in dialysis patients. Semin Dial 2007; 20: 139–143
17. Micheletti RG, Fishbein GA, Currier JS *et al.* Monckeberg sclerosis revisited: a clarification of the histologic definition of Monckeberg sclerosis. Arch Pathol Lab Med 2008; 132: 43–47
18. Schurgers LJ, Teunissen KJ, Knapen MH *et al.* Novel conformation-specific antibodies against matrix gamma-carboxyglutamic acid (Gla) protein: undercarboxylated matrix Gla protein as marker for vascular calcification. Arterioscler Thromb Vasc Biol 2005; 25: 1629–1633
19. Micheletti RG, Fishbein GA, Currier JS *et al.* Calcification of the internal elastic lamina of coronary arteries. Mod Pathol 2008; 21: 1019–1028
20. Wang N, Yang J, Yu X *et al.* Radial artery calcification in end-stage renal disease patients is associated with deposition of osteopontin and diminished expression of alpha-smooth muscle actin. Nephrology (Carlton) 2008; 13: 367–375
21. Toussaint ND. Extracellular matrix calcification in chronic kidney disease. Curr Opin Nephrol Hypertens 2011; 20: 360–368
22. Kendrick J, Chonchol M. The role of phosphorus in the development and progression of vascular calcification. Am J Kidney Dis 2011; 58: 826–834
23. Pai A, Leaf EM, El-Abbadi M *et al.* Elastin degradation and vascular smooth muscle cell phenotype change precede cell loss and arterial medial calcification in a uremic mouse model of chronic kidney disease. Am J Pathol 2011; 178: 764–773
24. Jono S, McKee MD, Murry CE *et al.* Phosphate regulation of vascular smooth muscle cell calcification. Circ Res 2000; 87: E10–E17
25. Li X, Yang HY, Giachelli CM. Role of the sodium-dependent phosphate cotransporter, Pit-1, in vascular smooth muscle cell calcification. Circ Res 2006; 98: 905–912
26. Di Marco GS, Hausberg M, Hillebrand U *et al.* Increased inorganic phosphate induces human endothelial cell apoptosis in vitro. Am J Physiol Renal Physiol 2008; 294: F1381–F1387
27. Mansfield K, Pucci B, Adams CS *et al.* Induction of apoptosis in skeletal tissues: phosphate-mediated chick chondrocyte apoptosis is calcium dependent. Calcif Tissue Int 2003; 73: 161–172
28. Proudfoot D, Skepper JN, Hegyi L *et al.* Apoptosis regulates human vascular calcification in vitro: evidence for initiation of vascular calcification by apoptotic bodies. Circ Res 2000; 87: 1055–1062
29. Stubbs JR, Liu S, Tang W *et al.* Role of hyperphosphatemia and 1,25-dihydroxyvitamin D in vascular calcification and mortality in fibroblastic growth factor 23 null mice. J Am Soc Nephrol 2007; 18: 2116–2124
30. Tamei N, Ogawa T, Ishida H *et al.* Serum fibroblast growth factor-23 levels and progression of aortic arch calcification in non-diabetic patients on chronic hemodialysis. J Atheroscler Thromb 2011; 18: 217–223
31. Goetz R, Nakada Y, Hu MC *et al.* Isolated C-terminal tail of FGF23 alleviates hypophosphatemia by inhibiting FGF23-FGFR-Klotho complex formation. Proc Natl Acad Sci USA 2010; 107: 407–412
32. Sprecher E. Familial tumoral calcinosis: from characterization of a rare phenotype to the pathogenesis of ectopic calcification. J Invest Dermatol 2010; 130: 652–660
33. Lyles KW, Halsey DL, Friedman NE *et al.* Correlations of serum concentrations of 1,25-dihydroxyvitamin D, phosphorus, and parathyroid hormone in tumoral calcinosis. J Clin Endocrinol Metab 1988; 67: 88–92
34. Larsson T, Yu X, Davis SI *et al.* A novel recessive mutation in fibroblast growth factor-23 causes familial tumoral calcinosis. J Clin Endocrinol Metab 2005; 90: 2424–2427
35. Chefetz I, Ben Amitai D, Browning S *et al.* Normophosphatemic familial tumoral calcinosis is caused by deleterious mutations in SAMD9, encoding a TNF-alpha responsive protein. J Invest Dermatol 2008; 128: 1423–1429
36. Masi L, Gozzini A, Franchi A *et al.* A novel recessive mutation of fibroblast growth factor-23 in tumoral calcinosis. J Bone Joint Surg Am 2009; 91: 1190–1198
37. Takada I, Mihara M, Suzawa M *et al.* A histone lysine methyltransferase activated by non-canonical Wnt signalling suppresses PPAR-gamma transactivation. Nat Cell Biol 2007; 9: 1273–1285
38. Rubin MR, Silverberg SJ. Vascular calcification and osteoporosis—the nature of the nexus. J Clin Endocrinol Metab 2004; 89: 4243–4245
39. Bhatt PM, Lewis CJ, House DL *et al.* Increased Wnt5a mRNA expression in advanced atherosclerotic lesions, and oxidized LDL treated human monocyte-derived macrophages. Open Circ Vasc J 2012; 5: 7
40. Bucay N, Sarosi I, Dunstan CR *et al.* osteoprotegerin-deficient mice develop early onset osteoporosis and arterial calcification. Genes Dev 1998; 12: 1260–1268
41. Min H, Morony S, Sarosi I *et al.* Osteoprotegerin reverses osteoporosis by inhibiting endosteal osteoclasts and prevents vascular calcification by blocking a process resembling osteoclastogenesis. J Exp Med 2000; 192: 463–474

Received for publication: 9.4.2014; Accepted in revised form: 27.8.2014